

Remote-sensing gas measurements with coherent Rayleigh-Brillouin scattering

A. Gerakis,^{1,a)} M. N. Shneider,² and B. C. Stratton¹

¹Princeton Plasma Physics Laboratory, 100 Stellarator Road, Princeton, New Jersey 08540, USA

²Department of Mechanical and Aerospace Engineering, Princeton University, Princeton, New Jersey 08540, USA

(Received 6 May 2016; accepted 13 July 2016; published online 21 July 2016)

We measure the coherent Rayleigh-Brillouin scattering (CRBS) signal integral as a function of the recorded gas pressure in He, CO₂, SF₆, and air, and we confirm the already established quadratic dependence of the signal on the gas density. We propose the use of CRBS as an effective diagnostic for the remote measurement of gas' density (pressure) and temperature, as well as polarizability, for gases of known composition. *Published by AIP Publishing.*

[<http://dx.doi.org/10.1063/1.4959778>]

Since its initial demonstration,^{1,2} Coherent Rayleigh-Brillouin Scattering (CRBS) has demonstrated the ability to measure important thermodynamic quantities in a gas or gas mixture, such as its temperature, speed of sound, and shear and bulk viscosity.³⁻⁸

Compared to Spontaneous Rayleigh-Brillouin Scattering (SRBS), in which the signal is scattered in a 4π solid angle, CRBS has the important advantage that the scattered signal is a coherent laser beam, allowing for measurements at a distance without a decrease in the signal to noise ratio (SNR). As a result of it being a four wave mixing process and the phasematching conditions, it offers a high degree of spatial localization, typically 100–200 μm . Utilizing the chirped lattice CRBS approach⁹ allows spectral acquisition times of 150 ns to be achieved. Finally, in SRBS, the intensity of the scattered light, I_S , is linearly proportional to the number of scatterers N . In contrast, the CRBS signal intensity I_S is proportional to the square of the induced refractive index modulation: $I_S \propto L^2(\Delta N)^2 I_1 I_2 I_{pr} \propto \Delta n^2$, where I_1 and I_2 are the pump intensities, I_{pr} the probe intensity, and $\Delta n = \frac{\alpha_{eff} \Delta N}{2\epsilon_0}$, with α_{eff} being the effective polarizability of the gas particles (atoms or molecules) and ΔN the induced periodic density modulation.

Confirmation of this quadratic dependence would allow CRBS signal calibration for a known gas composition and pressure. This would allow extrapolation of the measured CRBS signal for gases with unknown pressures and would enable the use of CRBS for remote pressure measurement in atomic gases, molecular gases, or a mixture of gases at a known and constant composition. The N^2 (and thus p^2 since $p = nk_B T$, where p is the pressure, T is the temperature, and n is the number density equal to $n = N/V$, where V is the volume) dependence of the CRBS signal has already been demonstrated in Ref. 10 for N₂ and here we offer comprehensive validation of this dependence for a number of different gases. We believe that the method described can be an important tool for accurate, remote, and non-intrusive pressure and temperature measurements. Additionally, measuring the CRBS signal intensities for different gases at the

same pressure allowed us to confirm the dependence of the CRBS signal intensity on the gas polarizability, as predicted in Ref. 11, thus demonstrating how the effective polarizability of a gaseous medium can be accurately estimated using CRBS.

Remote, non-perturbing measurements of gas parameters are of great utility to experimental fluid dynamics and aerodynamics, as well as other research areas. A diagnostic method that fulfills these criteria would be a significant improvement on perturbative gauges to measure the gas pressure, such as Pitot tubes, and would eliminate the need for the use of a gas cell in static pressure systems.

CRBS is a four-wave mixing technique in which two laser beams (called the *pumps*) of set frequency difference $\Delta\omega$ and of wavelength λ_{pump} interfere within a medium to create, due to electrostriction, an optical lattice of wavelength $\lambda_g = \lambda_{pump}/(2 \sin \phi)$ and of phase velocity v given by $v = (\omega_1 - \omega_2)/(\mathbf{k}_1 - \mathbf{k}_2) = (\Delta\omega \cdot \lambda_{pump})/(2 \cdot \sin \phi)$, where ϕ is the half angle between the two pump beams (Fig. 1). If a

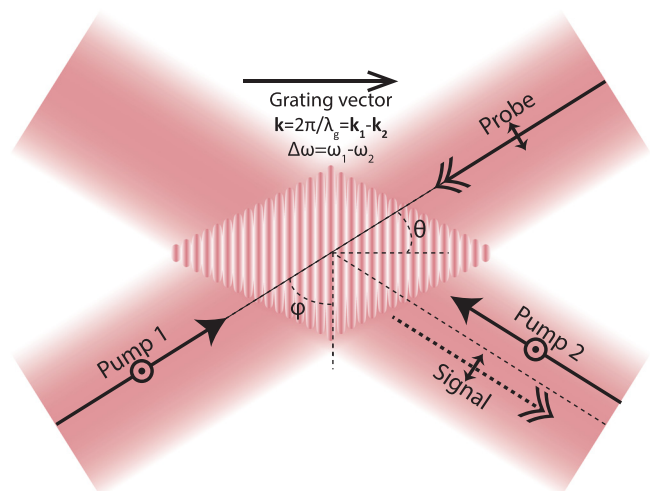


FIG. 1. Schematic of a typical CRBS geometry. Two almost counter-propagating, equipolarized pump beams cross within a medium at a half-angle ϕ to create an optical lattice. A probe beam, normally polarized to the pumps, is incident at this lattice at the Bragg angle θ and is being scattered from it producing a signal beam, which maintains all the spatial and polarization characteristics of the probe beam.

^{a)}Electronic mail: agerakis@pppl.gov

third beam (called the *probe*) of wavelength λ_{probe} is incident upon this lattice at the Bragg angle $\theta = \sin^{-1}(\lambda_{probe}/(2 \cdot \lambda_g))$, then a fourth coherent beam, called the *signal*, is generated. The CRBS spectrum is the record of the intensity of the signal beam with respect to $\Delta\omega$ and it consists of three distinct peaks. One is the Rayleigh peak, centered around $\Delta\omega = 0$, which is Doppler broadened due to the thermal motion of the medium. Equally shifted around it and centered at the speed of sound are the two Brillouin peaks due to acoustic (pressure) waves launched in the medium.

The CRBS experiment used in this work is shown in Fig. 2. The laser system is largely based on the setup used in Ref. 9. Therefore, we provide only a short description of it here. The ~ 15 mW single-mode, continuous-wave (CW) output of a custom made Nd:YVO₄ microchip laser (called the *master*), which hosts an intracavity LiTaO₃ electro-optic modulator (EOM), is injection seeded on a commercial laser diode emitting ~ 20 mW, single-mode at 1064 nm (called the *slave*). The output of the slave is further amplified to 1 W by a commercial fiber amplifier (IPG Photonics YAR-1 K-1064-LP-SF). This CW beam is then split into two, and the resulting beams propagate through two intensity modulators (Jenoptik AM1064b) which chop the CW beams into pulses. When the first pulse has passed through the intensity modulator, a voltage signal is sent to the master laser's EOM in order to change the frequency of the second pulse with respect to the first one. When the resulting two pulses interfere, they create chirped optical lattices within a medium. The two pulses are further amplified through two custom made, triple stage, diode-pumped ND:YAG amplifiers. With this system, we obtain flat-top pulses of 10–1000 ns duration, with measured energies up to 250 mJ/pulse and chirps exceeding 1 GHz. Since the CRBS spectral range is inversely proportional to the molecular weight and dependent on the scattering angle, larger chirp rates may be needed to measure the CRBS profiles of lighter particles.

The main advantage of this setup compared to other CRBS implementations is that, by employing chirped optical

lattices, i.e., lattices in which $\Delta\omega$ is chirped for the duration of the pulse, it allows for a very fast acquisition of a CRBS spectrum in a single laser pulse. By comparison, it takes conventional CRBS implementations between 5 and 20 min for the acquisition of a CRBS spectrum.

Part of both beams is heterodyned on a fast photodiode (Hamamatsu Photonics G6854–01), and we use the analysis technique of Fee *et al.*¹² to determine the instantaneous frequency $f(t)$ of the beat signal across the pulse duration. The temporal spread of the resulting CRBS profile will be a function of the temporal profile of the induced chirp. A linear chirp rate is then preferential since the effective phase velocity is linearly mapped with the chirp rate. The heterodyne detection we are performing aids to verify, and correct if necessary, the chirp we are inducing. This way, we can determine the effective phase velocity across the pulse duration. The probe beam is derived from pump 1 through a thin film polarizer (TFP), and thus its polarization is normal to that of the pumps and it does not interfere with them. All beams have an energy of ~ 130 mJ/pulse and a duration of ~ 200 ns which, when focused to a spot of ~ 150 μm diameter, corresponds to an intensity of $\sim 1.2 \times 10^{14}$ W m^{-2} .

The signal beam counterpropagates pump 2 and is separated from it through a TFP since it retains the polarization of the probe. It propagates for a long distance (8–10 m) in order to minimize the contribution of background light, before it is being detected. Since CRBS is a coherent process, the contribution of any incoherent components to the signal will decrease quadratically with distance. At high pressures, the signal is strong enough to be detected via a simple CCD camera (Thorlabs DCC1545M). This is the detector used for an initial optimization of the CRBS signal after which, a fast, unamplified photodiode (Hamamatsu Photonics G6854–01) can be used to spectrally resolve the CRBS signal on the oscilloscope. Figure 3 presents the CRBS signal averaged over 20 pulses from SF₆ gas, at atmospheric pressure and room temperature. There is almost perfect agreement between the spectral location of the Brillouin

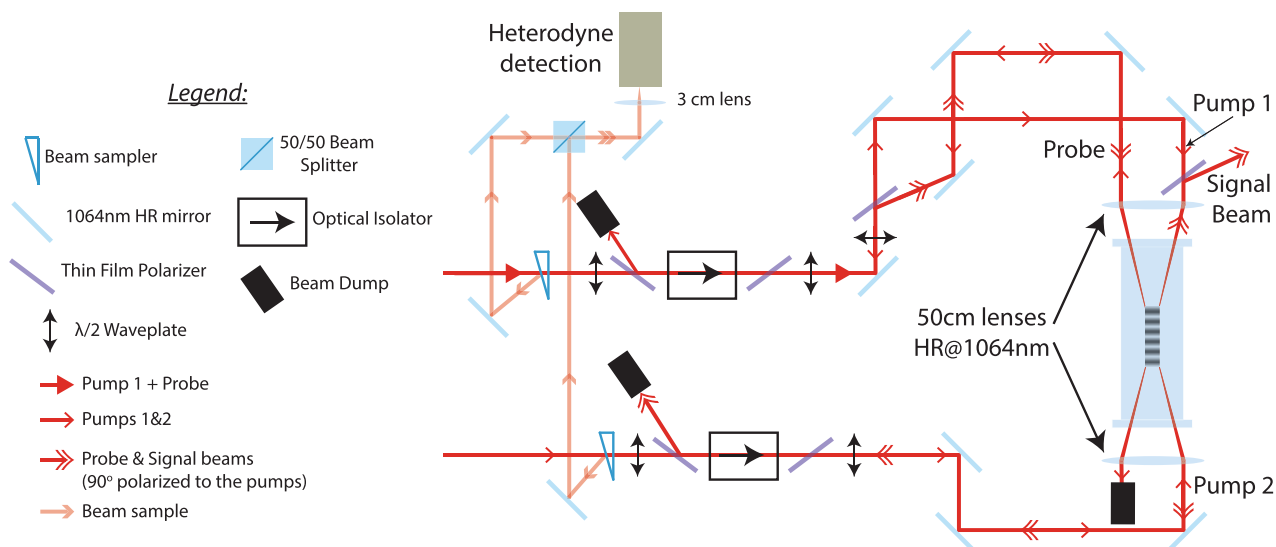


FIG. 2. Beam layout of the CRBS geometry used. The probe beam is derived from pump 1 via a thin film polarizer (TFP) and thus its polarization is normal to the pumps. The three beams are focussed through two lenses of 50 cm focal length and cross in the center of a gas cell. The generated signal beam counterpropagates pump 1 and is being separated from it via a TFP.

peaks and the speed of sound in SF₆, allowing us to be confident about the validity of the CRBS spectrum.

For low intensity measurements, the unamplified photodiode is replaced with an avalanche photodiode (APD). The APD used (Hamamatsu C5460-01) has a low bandwidth, resulting in a slow response (on the order of a few μ s) which does not allow spectral resolution of the CRBS spectrum as was the case with the unamplified photodiode. However, we can record the integral of the signal, which is linearly proportional to the signal intensity, thus not altering the calibration procedure. This allows us to verify the N^2 dependence of the integrated signal, similar to the verification of the integrated signal being proportional to N in spontaneous Rayleigh scattering.¹³

Figure 4 is a plot of the recorded values of the CRBS spectrally integrated signal for various pressures and for four different gases as measured with the APD, with the background subtracted for each data point. Also plotted is the quadratic fit to each experimental curve, normalized to the largest experimental value, in order to illustrate the quadratic dependence of the CRBS signal intensity with respect to pressure. It is apparent that there is ideal quadratic dependence of the measured signal with respect to pressure for all gases, confirming the findings in Ref. 10. A small disagreement can only be observed at very low signal levels (for air and CO₂, inset of Fig. 4), which is attributed to the gain nonlinearity of the APD at low signal levels. Consequently, we propose that CRBS can be used for an accurate measurement of gas pressure in environments where one cannot simply use a pressure gauge, such as in combustion and transient flow environments. If one calibrates the measurement system at a known pressure, then one can measure at an area of unknown pressure and extrapolate the pressure with relative ease, with an estimated error of $\sim 5\%$

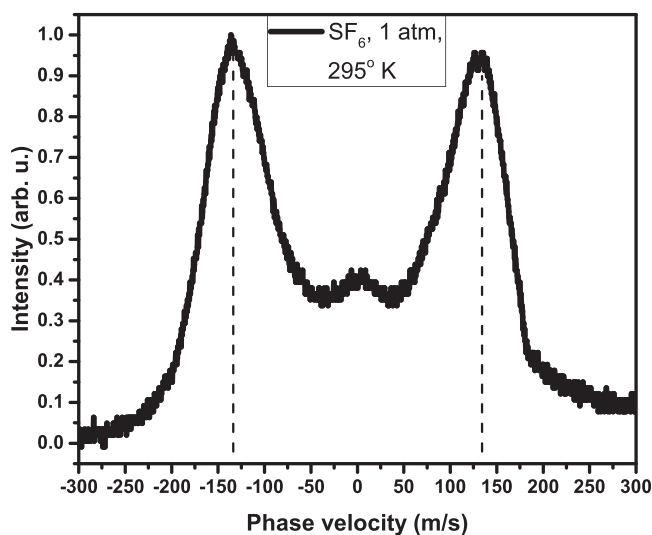


FIG. 3. Single shot CRBS spectrum obtained through the unamplified photodiode for SF₆ gas at room temperature and a pressure of 1 atm. The black dashed line indicates the speed of sound in SF₆ for these conditions as obtained from NIST tables (133.81 ms^{-1} at 293 K and pressure of 1 atm). The speed of sound from the obtained CRBS spectrum is found by fitting a Gaussian curve on each of the Brillouin peaks. The discrepancy between the NIST and our measured values is $\sim 2.3 \pm 0.7\%$, demonstrating the ability to accurately measure the speed of sound and hence the temperature in a medium of known composition.

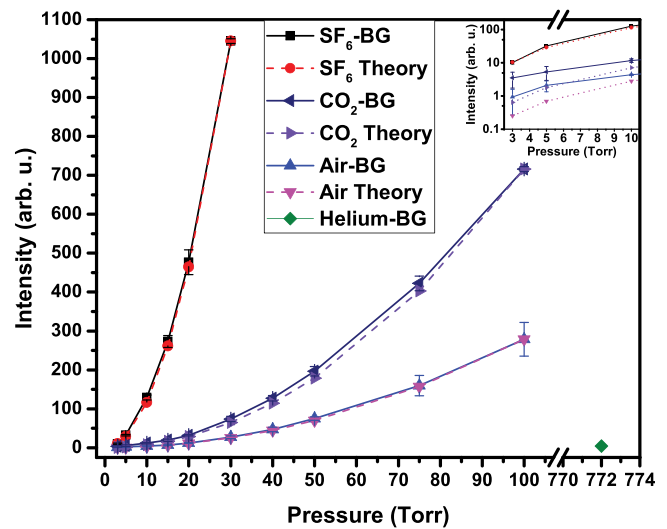


FIG. 4. Plots of the recorded CRBS spectral integrals for SF₆, CO₂, air, and He gases at various pressures (solid lines). Each data point represents the average of three measurements performed under the same conditions. The dashed lines are the quadratic fits to each experimental curve, normalized to the highest value per curve. The inset on the top right corner is a zoomed in version of the main plot, for the low pressure range, in a logarithmic intensity scale. BG denotes the background. Pressure is recorded with capacitance manometers while the background is recorded with the cell at a pressure of 10 mTorr (MKS 622C and MKS 122B, for 0–10 Torr and 10–1000 Torr, respectively). The error bars originate from the standard deviation of three different measurements performed under the same experimental conditions.

as it emerges from the error bars in Fig. 4. Additionally, given the high spatial resolution of CRBS, typically between 100 and 200 μ m, one can expect that this method could potentially be utilized for mapping out pressure in turbulent and laminar flows. Furthermore, as Fig. 4 suggests, the method is applicable to both molecular and atomic gases, as well as gas mixtures. The only constraint for the validity of the method would be that, for a gas mixture, the ratio of the constituent gases has to remain unchanged.

Another important finding from Fig. 4 is also the difference in scattering intensities for the different gases we measured at the same pressure. Indeed, since for the induced refractive index modulation Δn it holds that $\Delta n \propto \alpha_{eff}^{2-2.5}$ it would follow for the ratio of the scattered intensities from two different gases at the same pressure, that $N_1/N_2 \propto (\alpha_{eff2}/\alpha_{eff1})^{5/2}$, as shown in Ref. 11 for optimal conditions, i.e., for when the phase velocity is optimal for the density perturbation of the i -th component and equal to $\sqrt{kT/M_i}$, where M_i is the molecular mass. So for the SF₆, CO₂, air, and He gases we measured, with respective polarizabilities of 6.54, 2.507, 1.834 (effective), and 0.2 (all in units of $10^{-40} \text{ C m}^2 \text{ V}^{-1}$), it is expected that the acquired signal intensity between two gases at a particular pressure would scale as the ratio of the polarizabilities to the same power. Hence, we have demonstrated the use of CRBS as a tool to validate and specify the effective polarizability in a gas, and more importantly a gas mixture, using another gas of established polarizability as a reference.

To date, the main efforts to provide such a pressure measurement tool have concentrated on the application of laser-induced thermal-acoustics (LITA) and laser-induced thermal grating spectroscopy (LITGS).¹⁴⁻¹⁹ Although these methods

have successfully demonstrated their applicability in pressure and temperature measurement, they do have some limitations. More specifically, because they are dependent on the laser radiation absorption and subsequent acoustic wave generation, they work well at high pressures (typically above 2 atm) while only one such method has demonstrated its applicability at a pressure below 100 Torr.¹⁷ Finally, although the temperature measurement is trivial with these techniques (for a known gas composition), pressure derivation is in general model dependent and computationally complex and expensive, since it is derived from the fit to the obtained experimental data.¹⁵

We have verified for a range of gases the already established quadratic dependence of the obtained CRBS signal intensity on the gas density and thus pressure if the temperature is known. We have also shown that CRBS can be used for the measurement of temperature at high pressures by the spectral position of the Brillouin peaks since $v_{\text{sound}} = \sqrt{\frac{\gamma RT}{M}}$ where γ is the adiabatic constant and M is the molecular mass of the gas. At low pressures, where the Brillouin peaks cannot be observed, the temperature can be derived by the lineshape of the Rayleigh peak as shown in previous works.¹⁻³ Consequently, we have shown how this method can be used for remote, nonintrusive pressure, temperature and polarizability measurements in a gas or gas mixture of known composition. Of course, temperature and pressure cannot be simultaneously measured since one of these quantities is needed for the other to be retrieved. The results reported in the present letter are in agreement and in accordance with previous studies in the literature, in which accurate measurements of temperature in atomic and molecular gases,⁴ flames²⁰ and weakly ionized plasmas²¹ as well as bulk viscosity^{7,8,22} and speed of sound⁶ have been reported. We have thus added pressure and polarizability in the list of quantities that can be measured with CRBS and, if one follows the chirped lattice approach shown here, shown how almost the full state of the free gas can be measured in a single laser pulse. Finally, it should be mentioned that measure-

ments at pressures below 5 Torr should be possible using an APD with higher quantum efficiency than used here.

The authors would like to thank Dr. Y. Raitzes and Dr. K. Hara of Princeton Plasma Physics Laboratory and Dr. A. Dogariu of Department of Mechanical and Aerospace Engineering, Princeton University for useful discussions. This work was supported by the U.S. Department of Energy, Office of Science, Basic Energy Sciences, Materials Sciences and Engineering Division. The digital data for this paper can be found at <http://arks.princeton.edu/ark:/88435/dsp01x920g025r>.

- ¹J. H. Grinstead and P. F. Barker, *Phys. Rev. Lett.* **85**, 1222 (2000).
- ²X. Pan, M. N. Shneider, and R. B. Miles, *Phys. Rev. Lett.* **89**, 183001 (2002).
- ³X. Pan, M. N. Shneider, and R. B. Miles, *Phys. Rev. A* **69**, 033814 (2004).
- ⁴J. Gaul and T. Lilly, *Opt. Express* **22**, 20117 (2014).
- ⁵B. M. Cornella, S. F. Gimelshein, M. N. Shneider, T. C. Lilly, and A. D. Ketsdever, *Opt. Express* **20**, 12975 (2012).
- ⁶A. Gerakis, M. N. Shneider, and P. F. Barker, *Opt. Express* **19**, 24046 (2011).
- ⁷M. O. Vieitez, E. J. van Duijn, W. Ubachs, B. Witschas, A. Meijer, A. S. de Wijn, N. J. Dam, and W. van de Water, *Phys. Rev. A* **82**, 043836 (2010).
- ⁸A. S. Meijer, A. S. de Wijn, M. F. E. Peters, N. J. Dam, and W. van de Water, *J. Chem. Phys.* **133**, 164315 (2010).
- ⁹A. Gerakis, M. N. Shneider, and P. F. Barker, *Opt. Lett.* **38**, 4449 (2013).
- ¹⁰T. Lilly, A. Ketsdever, B. Cornella, T. Quiller, and S. Gimelshein, *Appl. Phys. Lett.* **99**, 124101 (2011).
- ¹¹M. N. Shneider and S. F. Gimelshein, *Appl. Phys. Lett.* **102**, 173109 (2013).
- ¹²M. S. Fee, K. Danzmann, and S. Chu, *Phys. Rev. A* **45**, 4911 (1992).
- ¹³R. B. Miles, W. R. Lempert, and J. N. Forkey, *Meas. Sci. Technol.* **12**, R33 (2001).
- ¹⁴E. B. Cummings, *Opt. Lett.* **19**, 1361 (1994).
- ¹⁵R. Stevens and P. Ewart, *Appl. Phys. B* **78**, 111 (2004), ISSN: 1432-0649.
- ¹⁶R. C. Hart, G. C. Herring, and R. J. Balla, *Opt. Lett.* **27**, 710 (2002).
- ¹⁷R. C. Hart, G. C. Herring, and R. J. Balla, *Opt. Lett.* **32**, 1689 (2007).
- ¹⁸F. J. Förster, S. Baab, G. Lamanna, and B. Weigand, *Appl. Phys. B* **121**, 235 (2015), ISSN: 1432-0649.
- ¹⁹A. Hell, F. J. Förster, and B. Weigand, "Validation of laser-induced thermal acoustics for chemically reacting H₂/air free jets," *J. Raman Spectrosc.* (published online 2016).
- ²⁰H. T. Bookey, A. I. Bishop, and P. F. Barker, *Opt. Express* **14**, 3461 (2006).
- ²¹X. Pan, P. F. Barker, A. Meschanov, J. H. Grinstead, M. N. Shneider, and R. B. Miles, *Opt. Lett.* **27**, 161 (2002).
- ²²X. Pan, M. Shneider, Z. Zhang, and R. Miles, "Bulk viscosity measurements using coherent Rayleigh-Brillouin scattering," AIAA Paper No. 17, 2004.